Stem Cell Reports, Volume *16*

Supplemental Information

Progesterone receptor-DNA methylation crosstalk regulates depletion of uterine leiomyoma stem cells: A potential therapeutic target

Shimeng Liu, Ping Yin, Jingting Xu, Ariel J. Dotts, Stacy A. Kujawa, John S. Coon V, Hong Zhao, Yang Dai, and Serdar E. Bulun

Supplemental Material

Supplemental Figures and Legends

Figure S1

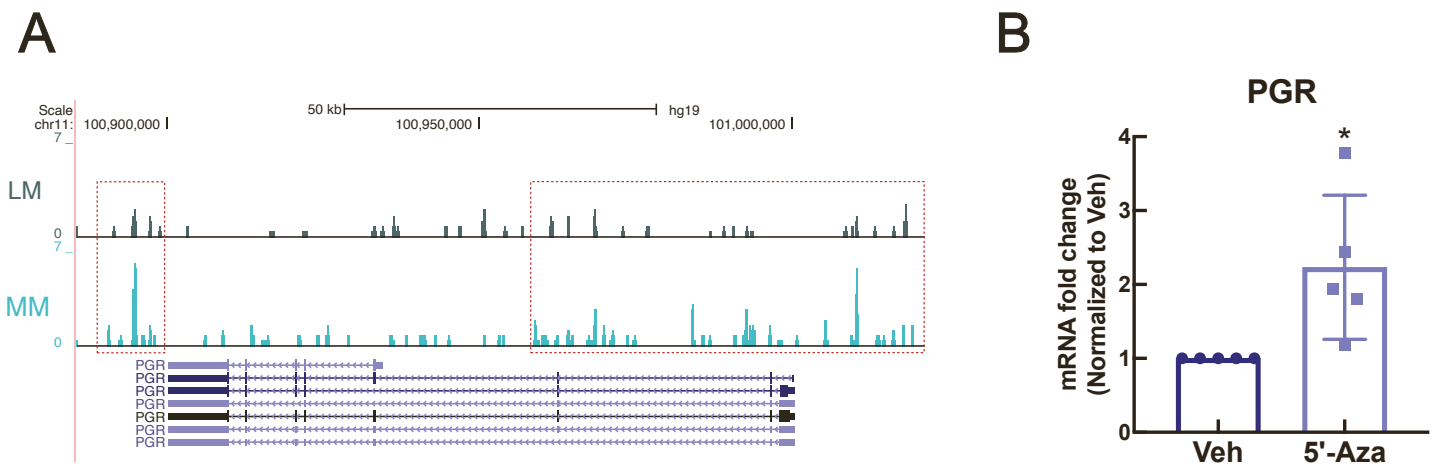

Figure S1. 5′-Aza regulates PGR gene expression in myometrium. [Related to Figure 1]

A) Representative genome browser view showing methylation status around the *PGR* gene locus in LM and myometrium (MM) tissue. **B**) Bar graph showing real-time qPCR results of PGR mRNA levels in primary MM cells treated with 5′-Aza (100 nM) or vehicle (DMSO) for 96 h (n = 5 patients, **P*<0.05, t-test).

Figure S2

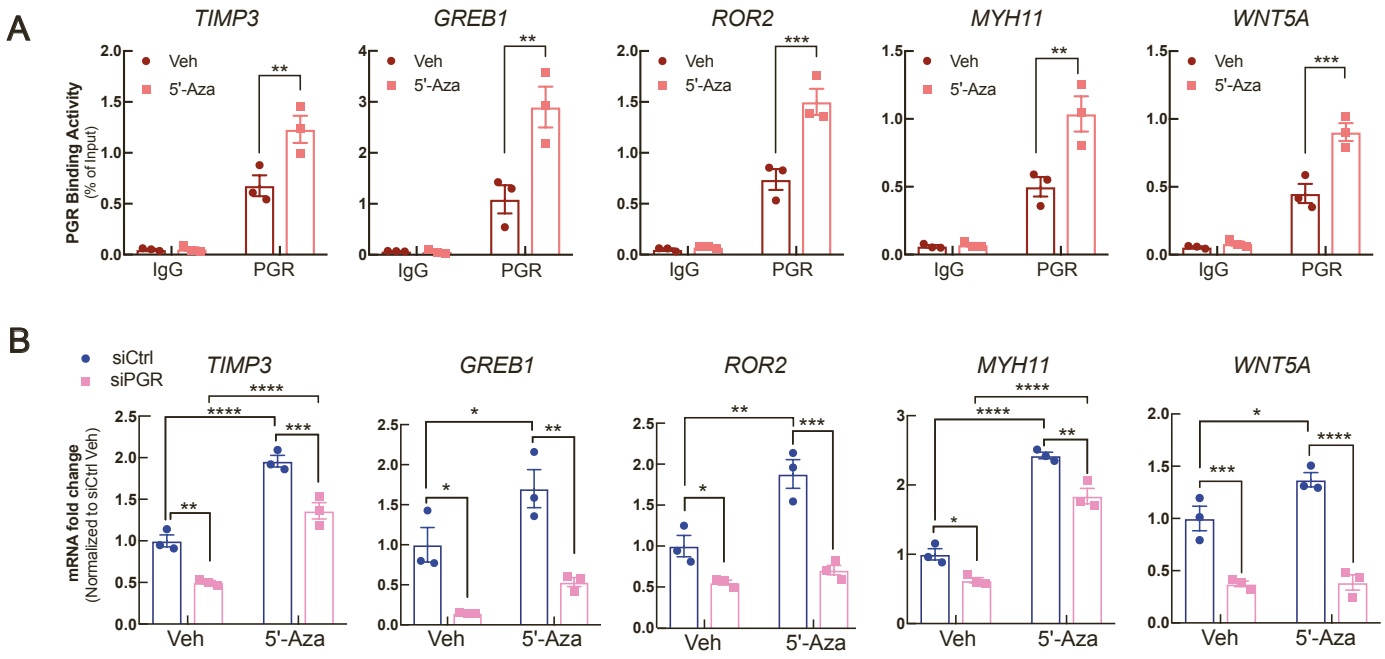

Figure S2. PGR signaling activity is activated by 5′-Aza. [Related to Figure 2]

A) ChIP-qPCR showing PGR recruitment to PGR-binding sites adjacent to the differentially methylated regions around the PGR target genes in primary LM cells exposed to vehicle (DMSO) or 5′-Aza (96 h, 100 nM) (means ± SEM, n = 3 patients, ***P*<0.01, ****P*<0.001, two-way ANOVA). Samples were treated with R5020 (10^{-7} M) for 1 hour before harvesting for ChIP. **B**) Bar graphs showing mRNA levels of PGR target genes in siCtrl- and siPGR1-transfected (50 nM) primary LM cells with or without 5′-Aza treatment (6 days, 100 nM; means ± SEM, n = 3 patients, **P*<0.05, ***P*<0.01, ****P*<0.001, *****P*<0.01, two-way ANOVA).

Figure S3

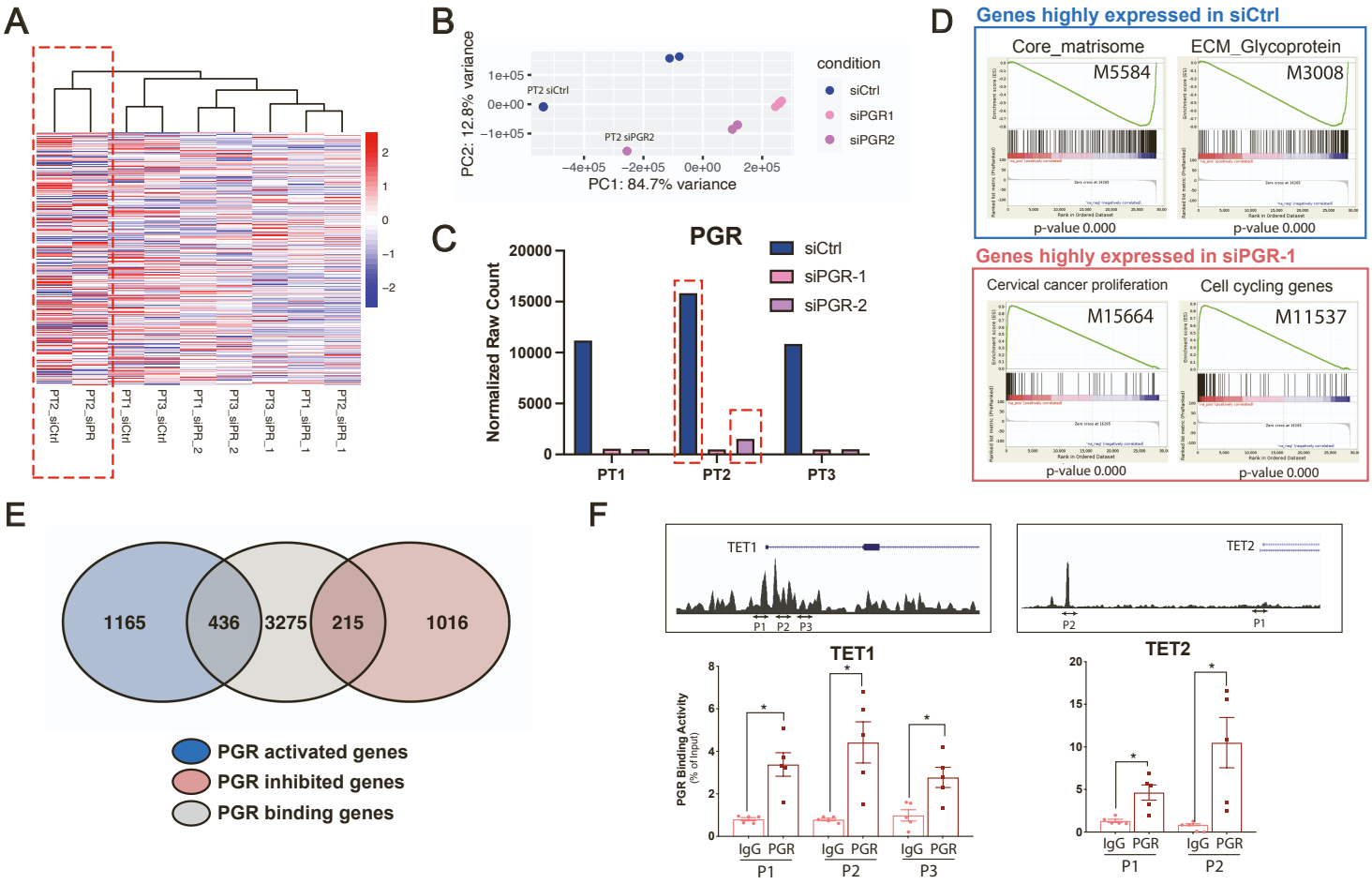

Figure S3. PGR regulates genes involved in LSC differentiation. [Related to Figure 3]

Heatmap (**A**) and PCA plot (**B**), which show transcriptome clustering of total LM primary cells transfected with siCtrl or siPGRs (n = 3 patients) based on the mRNA levels of the 4357 differentially expressed genes between LSC and LIC/LDC, identified PT2 as an outlier among 3 samples **C**) Normalized raw counts of PGR gene expression using RNA-seq data of LM cells transfected with siCtrl or siPGRs indicated that PGR gene expression was significantly higher in PT2 vs PT1 and PT3. **D**) Gene set enrichment analysis (GSEA) of siCtrl and siPGR-1 RNA-Seq

data in **Figure 3B** based on C2 (curated gene sets) collection in the GSEA database. Top and bottom panels represent pathways of genes highly expressed in siCtrl and siPGR-1, respectively. **E**) Venn diagram showing overlapping genes between siPGR-regulated genes identified in **Figure 3C** and PGR-binding genes identified by PGR ChIP-Seq (n = 5 patients). **F**) PGR binding around *TET1* and *TET2* gene promoter regions in primary LM cells. Upper: Representative genome browser track view of PGR-binding sites retrieved from PGR ChIP-seq in LM tissue; Lower: ChIP-qPCR quantifying PGR enrichment around *TET1* and *TET2* gene promoter regions in primary LM cells (means ± SEM, n = 5 patients, **P*<0.05, paired t-test). P1, P2, and P3 indicate location of primers used for ChIP-qPCR.

Figure S4

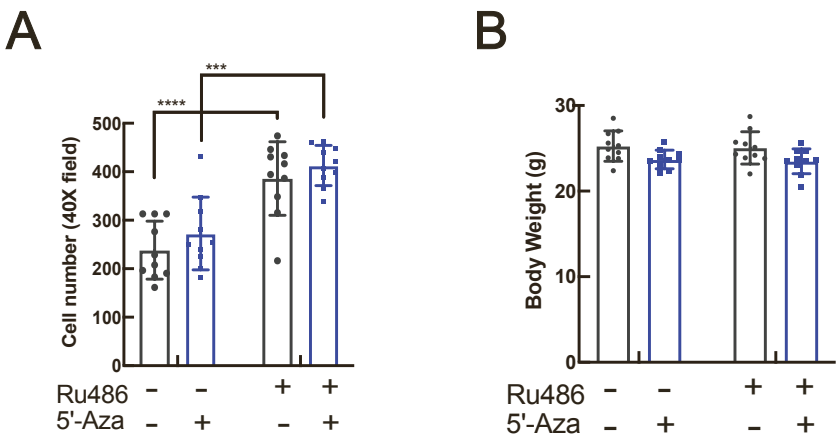

Figure S4. RU486 but not 5'-Aza treatment increased cell density in xenografted tumors. [Related to Figure 4]

A) Bar graph showing the average cell count in a 40x magnification field (n = 10 fields from 3 patients, ****P*<0.001, *****P*<0.01, two-way ANOVA). **B**) Bar graph showing mouse body weight in Figure 4A (no significant difference was detected among groups, two-way ANOVA).

Supplemental Tables

Supplemental Table 1. Antibody information

Antibody	Company	Cat. Number	Usage
CD45	BD Biosciences	564105	FACS
CD34	BD Biosciences	555824	FACS
CD49b	BD Biosciences	555498	FACS
PGR	Santa Cruz	sc-7208X	ChIP-qPCR/-Seq
Rabbit IgG	Cell signaling Tech	9003S	ChIP-qPCR
PGR	Dako Products (Agilent)	M3569	Western Blot
beta-actin	Proteintech	HRP-60008	Western Blot
Cyclin D1	Thermo Fisher Scientific	MA5-14512	IHC

Supplemental Table 2. ChIP-qPCR primer information

Name	Forward	Reverse	Chromasome coordinates (hg19)
WNT5A_PGR_binding	TCTTTGGAGCAGTCCCTTTG	GTGCCAACGTGCGTAGTTTA	Chr3: 55404352 - 55404521
TIMP3_PGR_binding	GATGAGAGATGGGCCTCAGA	AAATGTGCTCTCCCATCACC	Chr22: 33277141 - 33277294
ROR2_PGR_binding	CCACCAATGGGAACAAAAAG	TCCAGTGGAGGTGGTGTGTA	Chr9: 94635892 - 94635996
GREB1_PGR_binding	CACTTTGAGCAAAAGCCACA	GACCCAGTTGCCACACTTTT	Chr2: 11672557 - 11672663
MYH11_PGR_binding	TCTCGGAAAAGACCCAGCTA	GCACTGTTTGTCCCCTGATT	Chr16: 15949054 - 15949161
TET1_PGR_binding_P1	AGGTCCAGGGCCAAATAACT	AGAAGGTGCCAGGTCAGAGA	Chr10: 70319657 - 70319829
TET1_PGR_binding_P2	CAAGCGTACCCCCTAAACAA	TTCCCTTCTTCCCTGATCCT	Chr10: 70320982 - 70321178
TET1_PGR_binding_P3	CTGGGCATTTCTGATCCACT	ATTTGGGAGAGGGACGAGTT	Chr10: 70321593 - 70321696
TET2_PGR_binding_P1	TTCTCTTATGCCGCGAAACT	AGCTTCCCTCTTCCCTCTTG	Chr4: 106068147 - 106068265
TET2_PGR_binding_P2	TGTGTGGGAGTGGATTTTGA	GCCAAGGCATTAAATCCTGA	Chr4: 106013635 - 106013769

Supplemental Table 3. Expression primer information

Gene name	Company	Assay ID	Product Name
PGR	Life Technologies	Hs01556702_m1	TaqMan® Assays
TIMP3	Integrated DNA Technologies	Hs.PT.58.1756331	Predesigned qPCR Assays
GREB1	Integrated DNA Technologies	Hs.PT.58.26216464	Predesigned qPCR Assays
ROR2	Integrated DNA Technologies	Hs.PT.58.22908006	Predesigned qPCR Assays
MYH11	Integrated DNA Technologies	Hs.PT.58.2909933	Predesigned qPCR Assays
WNT5A	Integrated DNA Technologies	Hs.PT.58.22221435	Predesigned qPCR Assays
TET1	Integrated DNA Technologies	Hs.PT.58.27802060	Predesigned qPCR Assays
TET2	Integrated DNA Technologies	Hs.PT.58.21240322	Predesigned qPCR Assays
NANOG	Integrated DNA Technologies	Hs.PT.58.21480849	Predesigned qPCR Assays
KLF4	Integrated DNA Technologies	Hs.PT.58.45542593	Predesigned qPCR Assays
TBP	Life Technologies	Hs00427620_m1	TaqMan® Assays

Experimental Procedures

Tissue collection

Northwestern University's Institutional Review Board approved the use of human tissue. MM and LM tissues were obtained from 40 premenopausal women undergoing either myomectomy or hysterectomy (age 38 ± 9 years, range 29–47 years). We obtained informed consent from all participants. Patients receiving hormone treatment within 6 months prior to surgery were excluded. Tissues were dissociated and cells were isolated as previously described (Yin et al., 2015).

Primary cell culture

Primary MM and LM cells were maintained in Dulbecco's Modified Eagle's Medium (DMEM)/F12 (ThermoFisher Scientific, USA) containing 10% fetal bovine serum (FBS) and 1% antibiotic/antimycotic in a humidified atmosphere with 5% CO_2 at 37°C. All primary cells in this study were used within two passages.

Antibody-based cell sorting

As shown in Figure 1A, after singly dissociated from fresh tissue and incubated with fluorophore-conjugated antibodies against CD45, CD34, and CD49b, the cells were washed three times followed by incubation with propidium iodide (PI) to label non-viable cells. The cells were then sorted on a FACSAria cell sorter. The majority of cells were selected for analysis based on forward versus side scatter profile. Dead cells (PI^+) and leukocytes ($CD45^+$) were excluded by electronic gating. The remaining cells were sorted into three populations based on their expression of CD34 and CD49b: $CD34^-CD49b^-$, $CD34^+CD49b^-$, and $CD34^+CD49b^+$ cells (Ikhena et al., 2018; Yin et al., 2015).

Stem cell culture

Each freshly FACS-sorted population of LM cells was cultured in mesenchymal stem cell growth

medium (Lonza Bioscience, USA, PT-3238) in low-attachment 96-well plates (Fisher Scientific, USA, 07-201-680) to maintain stem cell characteristics. Cells were recovered in basal mesenchymal stem cell growth medium for 3 days and followed by treatment with 5′-Aza (100 nM) or vehicle (0.01% DMSO) for 96 hours.

PGR siRNA knockdown

LM passage zero cells were transfected with two different PGR siRNAs (Dharmacon, USA, D-003433-03-0010 and D-003433-01-0010) or control scrambled siRNA (D-001810-10-05) at 50 nM using Dharmafect 1 (Dharmacon, T-2001-02) transfection reagent. To determine the effect of PGR on 5′-Aza–mediated gene expression, after transfection for 24 hours, the cells were treated with 5′-Aza (100 nM) or vehicle for 6 days and R5020 (10^{-7} M) was added during the last 24 hours before harvesting for downstream analysis. For PGR knockdown followed by RNA-Seq analysis, the cells were transfected with PGR siRNA for 96 hours and R5020 (10^{-7} M) was added during the last 24 hours before harvesting for RNA-Seq.

RNA isolation, real-time qPCR, and RNA-Seq

Total RNA was isolated using the Qiagen Allprep RNA/DNA mini kit (Qiagen, Germany, 80204) or Qiagen RNeasy RNA micro kit (Qiagen, 74004). cDNA was synthesized using qScript cDNA SuperMix (total RNA >100 ng; VWR International, USA, 95048-100) or SuperScript VILO Master Mix (total RNA <100 ng; ThermoFisher Scientific, 11754050). mRNA levels were quantified using real-time qPCR normalized to TBP as previously described (Liu et al., 2019). Total RNA quality was examined using the Bioanalyzer: RNA Pico assay (Agilent, USA). RNA-Seq libraries were prepared using the NEBNext Ultra II RNA Library Prep with Sample Purification Beads (New England Biolabs, USA, 7775).

MethylCap-Seq

Genomic DNA was extracted from total LM cells after PGR knockdown using the Qiagen Allprep RNA/DNA mini kit (Qiagen, 80204), and fragmented to 300-500bp using Covaris M220 (Covaris, USA). Methylated DNA fragments were captured using the MethylCap Kit (Diagenode, USA, C02020010) following the manufacturer's protocol. Briefly, 500 ng of fragmented genomic DNA was incubated with H6-GST-MBD fusion proteins that can bind methylated cytosines. The protein-DNA complex was then precipitated with antibody-conjugated beads that are specific to the protein tag. The immunoprecipitated DNA fragments were purified and subjected to library construction and sequencing as described below (see **Next-generation sequencing**).

Chromatin immunoprecipitation assay

Previous studies demonstrate that the interaction of nuclear receptors (such as ESR1 and AR) with chromatin follows an on-and-off cyclical pattern (Kang et al., 2002; Métivier et al., 2003; Shang et al., 2000). To avoid the effects of in vitro tissue processing and cell isolation on PGR-chromatin interaction landscape, we immediately snap-froze fresh tissue in liquid nitrogen after surgery. 0.2-0.5 g of frozen LM tissues were used for ChIP-Seq. 5 X 10^6 passage zero LM cells were treated with R5020 for 1 hour before harvesting for ChIP-qPCR. Chromatin was isolated from LM tissue or cultured LM cells using the SimpleChIP Kit (Cell Signaling Technology, USA, 9005). 10 µg of chromatin was incubated with 3 µg anti-PGR antibody to immunoprecipitate DNA, which was purified for real-time qPCR or library preparation for next-generation sequencing described below. Normal rabbit IgG was used as a negative control.

Next-generation sequencing

Next-generation sequencing libraries for MethylCap-Seq and PGR ChIP-Seq were prepared using the KAPA Hyper Prep Kit (KAPA Biosystems, USA, KK8502) and KAPA Single-Indexed Adapter Kit (KAPA Biosystems, KK8710). The libraries were sequenced at the Northwestern

University NUSeq Core Facility using the NextSeq 500 system (Illumina, USA) with 20-40 million reads per sample. Sequencing methods were 50bp single-end for RNA-Seq, 75bp single-end for PGR ChIP-Seq, and 75bp paired-end for MethylCap-Seq.

Bioinformatic analysis

Sequences were aligned to the hg19 reference genome using TopHat for RNA-Seq, Bowtie2 for PGR ChIP-Seq and MethylCap-Seq, and Burrows-Wheeler Aligner (BWA) for histone modification ChIP-Seq (Kim et al., 2013; Langmead and Salzberg, 2012; Li and Durbin, 2009). Differential gene expression from RNA-Seq was detected using DESeq2 following the cutoff: FDR-adjusted $P<0.05$. We performed the following ChIP-Seq analyses using Homer: peak callings (-factor for PGR ChIP-Seq and -histone for MethylCap-Seq), overlapping region identifications (mergePeaks -d 100), motif analyses (findMotifsGenome.pl), and peak annotations (annotatePeaks.pl) (Heinz et al., 2010). Pathway enrichment analysis was performed using Metacore V6.34 (Thomson Reuters) and GSEA V4.0.1 (Mootha et al., 2003; Subramanian et al., 2005). Bam files from replicates were merged by samtools before NGSplot and UCSC Genome Browser visualizations (Hoekstra et al., 2009). Sequencing tracks were visualized using the UCSC Genome Browser. Visualization of DNA methylation and histone modification average levels at specified regions (PGR-binding regions and gene body regions) were performed using NGSplot (Shen et al., 2014). Hypermethylated PGR-binding regions in LSC were identified using the K-mean clustering option (-GO km, -KNC 5) included in NGSplot. Methylation levels at PGR-binding regions were quantified on bam files using normalized RPKM value ($\log2(RPKM_{IP}+1) - \log2(RPKM_{Input}+1)$).

Animal studies

Northwestern University's Animal Care and Use Committee approved all procedures involving animals in this study. 10^6 live cells were grafted underneath the kidney capsules of ovariectomized

nonobese diabetic-scid IL2Rgnull mouse hosts (NSG, Jackson Laboratory, USA) as previously described (Ikhena et al., 2018). To test the effect of 5′-Aza on the growth of existing tumors, 3 weeks after the tumor xenografts were established, mice were treated with vehicle or 5′-Aza (0.25 mg/kg, two intraperitoneal (*i.p*) injection /week) for 1 week. Then, the mice were subcutaneously implanted with placebo or a RU486 slow-release pellet (12.5 mg/pellet, 30-day release, SX-999, Innovative Research of America, USA) and the tumors were allowed to grow for another 2 weeks. Mice were euthanized 6 weeks post-surgery. Images of regenerated tumors on the kidney surface were taken from the x-, y-, and z-axes using a dissecting microscope connected to a computer with Leica Application Suite, version 3.8 software (Leica Microsystems Inc., Germany). Tumors were measured by two individuals who were blinded to the treatment group allocation; the average of the two measurements was used for data plotting. Tumor volume was quantified using the following formula: volume (mm^3) = 0.52 (derived from $\pi/6$) * length * width * height (mm^3) (Ishikawa et al., 2010).

Immunohistochemistry

Paraffin-embedded mouse kidneys xenografted with primary LM cells were sectioned and immunohistochemistry (IHC) was performed by the Northwestern University Histology and Phenotyping Laboratory to detect the proliferation marker Cyclin D1. Images were captured with a Leica microscope (Leica Microsystems Inc.). Cells stained positive for Cyclin D1 were counted in 40X fields by two individuals who were blinded to the treatment group allocation; the average of the counts by the two individuals were used for data plotting.

Immunoblot analysis

Protein was extracted from LM primary cells using radioimmunoprecipitation assay buffer, followed by quantification using bicinchoninic acid protein assay reagent (ThermoFisher Scientific,

23225) per the manufacturer's protocol. Total protein was diluted in reducing 4X LDS sample buffer (ThermoFisher Scientific, NP0007), electrophoresed on a 4% to 12% Novex Bis-Tris polyacrylamide precast gel (ThermoFisher Scientific, NP0321BOX), and transferred onto polyvinylidene difluoride membrane. Incubation with primary antibodies (Supplemental Table 1) was performed at 4°C in 5% nonfat milk overnight. The membranes were then washed and incubated with the appropriate horseradish peroxidase-conjugated secondary antibodies for 1 hour at room temperature. Detection was performed using Luminata Crescendo horseradish peroxidase substrate (Millipore, USA, WBLUR0100).

Statistical analysis

All statistical analyses were performed using GraphPad Prism 8 (GraphPad Inc.) and R (3.6.0). Paired Student's t-test was performed to compare the means between two treatment groups; One-way ANOVA followed by pairwise comparison analyses were performed to compare the means among three or more treatment groups; Two-way ANOVA followed by pairwise comparison analyses were performed to compare the means among treatment groups with two independent variables and to investigate the interaction between the two variables. Values were considered statistically significant when $P<0.05$. All experiments were repeated with samples from at least three patients, with the patient number (n) noted in the figure legends. Data points in the bar plots represent biological replicates from different patients or mice and error bars represent SEM.

Reference

Heinz, S., Benner, C., Spann, N., Bertolino, E., Lin, Y.C., Laslo, P., Cheng, J.X., Murre, C., Singh, H., and Glass, C.K. (2010). Simple combinations of lineage-determining transcription factors prime cis-regulatory elements required for macrophage and B cell identities. Mol Cell *38*, 576-589.

Hoekstra, A.V., Sefton, E.C., Berry, E., Lu, Z., Hardt, J., Marsh, E., Yin, P., Clardy, J., Chakravarti, D., Bulun, S.*, et al.* (2009). Progestins activate the AKT pathway in leiomyoma cells and promote survival. J Clin Endocrinol Metab *94*, 1768-1774.

Ikhena, D.E., Liu, S., Kujawa, S., Esencan, E., Coon, J.S.t., Robins, J., Bulun, S.E., and Yin, P. (2018). RANKL/RANK pathway and its inhibitor RANK-Fc in uterine leiomyoma growth. J Clin Endocrinol Metab *103*, 1842-1849.

Ishikawa, H., Ishi, K., Serna, V.A., Kakazu, R., Bulun, S.E., and Kurita, T. (2010). Progesterone is essential for maintenance and growth of uterine leiomyoma. Endocrinology *151*, 2433-2442.

Kang, Z., Pirskanen, A., Jänne, O.A., and Palvimo, J.J. (2002). Involvement of Proteasome in the Dynamic Assembly of the Androgen Receptor Transcription Complex*. Journal of Biological Chemistry *277*, 48366-48371.

Kim, D., Pertea, G., Trapnell, C., Pimentel, H., Kelley, R., and Salzberg, S.L. (2013). TopHat2: accurate alignment of transcriptomes in the presence of insertions, deletions and gene fusions. Genome Biol *14*, R36.

Langmead, B., and Salzberg, S.L. (2012). Fast gapped-read alignment with Bowtie 2. Nat Methods *9*, 357-359.

Li, H., and Durbin, R. (2009). Fast and accurate short read alignment with Burrows-Wheeler transform. Bioinformatics *25*, 1754-1760.

Liu, S., Yin, P., Kujawa, S.A., Coon, J.S.t., Okeigwe, I., and Bulun, S.E. (2019). Progesterone receptor integrates the effects of mutated MED12 and altered DNA methylation to stimulate RANKL expression and stem cell proliferation in uterine leiomyoma. Oncogene *38*, 2722-2735.

Métivier, R., Penot, G., Hübner, M.R., Reid, G., Brand, H., Koš, M., and Gannon, F. (2003). Estrogen Receptor-α Directs Ordered, Cyclical, and Combinatorial Recruitment of Cofactors on a Natural Target Promoter. Cell *115*, 751-763.

Mootha, V.K., Lindgren, C.M., Eriksson, K.F., Subramanian, A., Sihag, S., Lehar, J., Puigserver, P., Carlsson, E., Ridderstrale, M., Laurila, E.*, et al.* (2003). PGC-1alpha-responsive genes involved in oxidative phosphorylation are coordinately downregulated in human diabetes. Nat Genet *34*, 267-273.

Shang, Y., Hu, X., DiRenzo, J., Lazar, M.A., and Brown, M. (2000). Cofactor Dynamics and Sufficiency in Estrogen Receptor–Regulated Transcription. Cell *103*, 843-852.

Shen, L., Shao, N., Liu, X., and Nestler, E. (2014). ngs.plot: Quick mining and visualization of next-generation sequencing data by integrating genomic databases. BMC Genomics *15*, 284.

Subramanian, A., Tamayo, P., Mootha, V.K., Mukherjee, S., Ebert, B.L., Gillette, M.A., Paulovich, A., Pomeroy, S.L., Golub, T.R., Lander, E.S.*, et al.* (2005). Gene set enrichment analysis: a knowledge-based approach for interpreting genome-wide expression profiles. Proc Natl Acad Sci U S A *102*, 15545-15550.

Yin, P., Ono, M., Moravek, M.B., Coon, J.S.t., Navarro, A., Monsivais, D., Dyson, M.T., Druschitz, S.A., Malpani, S.S., Serna, V.A.*, et al.* (2015). Human uterine leiomyoma stem/progenitor cells expressing CD34 and CD49b initiate tumors in vivo. J Clin Endocrinol Metab *100*, E601-606.